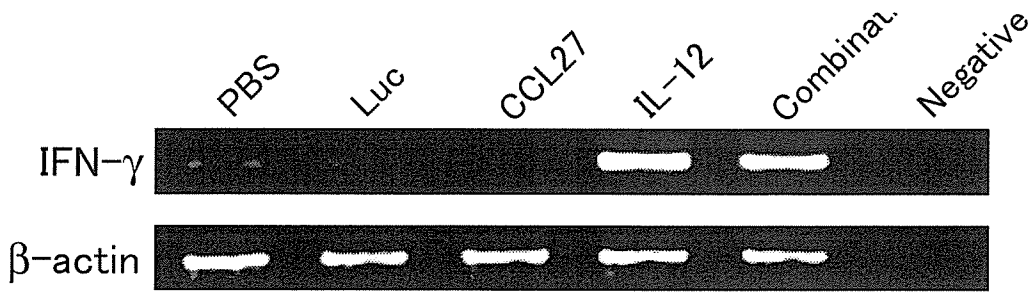

Fig. 13. RT-PCR analysis of murine IFN-γ in indicated adenovirus vectors injected OV-HM tumor nodules. Total RNA was extracted from OV-HM tumor nodules, and then RT-PCR was performed to amplify the mRNA levels of mouse IFN-γ (379bp) and β-actin (514bp). PCR products were visualized by ethidium bromide staining after electrophoresis on an agarose gel. Negative was performed PCR using water as template.

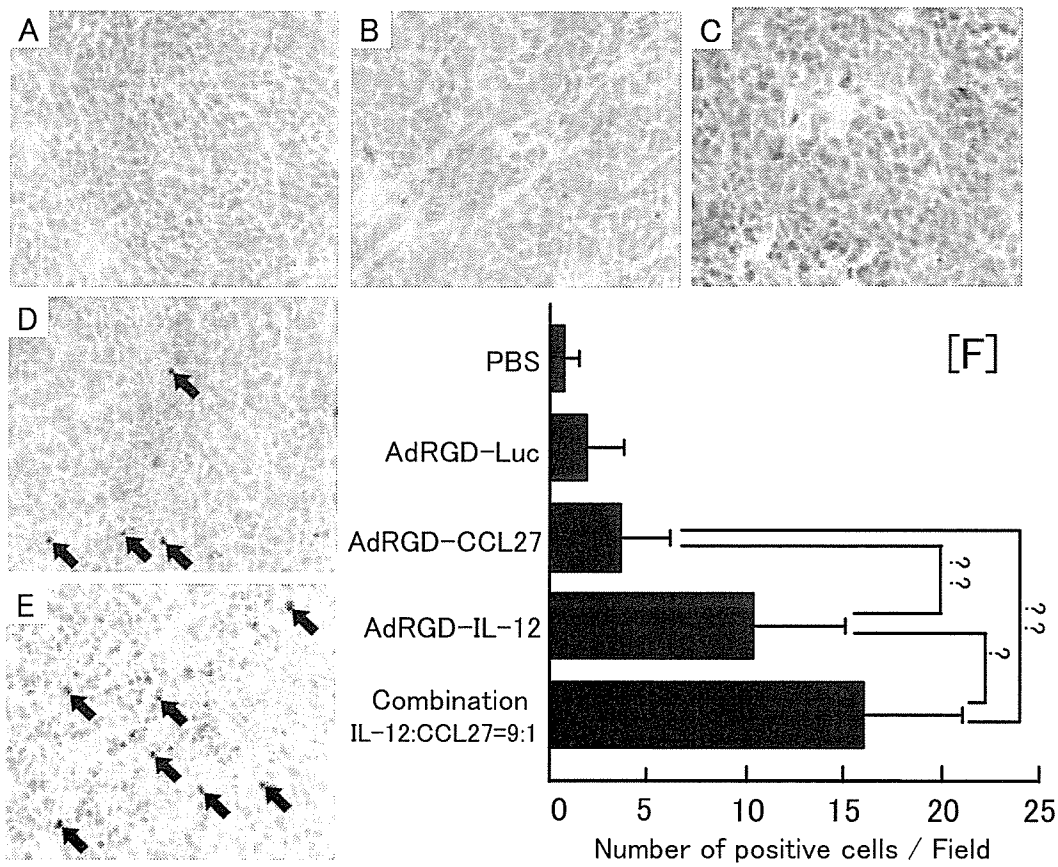

Fig. 14. Perforin positive cells infiltrate into OV-HM tumor. When the length of tumor reached about 7-8 mm, intratumoral administrations of indicated adenovirus vectors were carried out. Tumor-bearing mice were sacrificed in six days after the intratumoral administrations of (A) PBS, (B) AdRGD-Luc, (C) AdRGD-CCL27, (D) AdRGD-IL-12 and (E) combination (AdRGD-IL-12:AdRGD-CCL27=9:1). The tumor nodules were harvested, embedded in the O.C.T. compound, and stored at -80℃. Frozen thin sections of the nodules were fixed and stained for perforin-positive cells using the method described above. The number of immunostained cells were counted under light microscope with ×400 magnification. For counting the positive cell number infiltrated into tumor tissue, 6 fields were randomly selected. (F) Quantitation of perforin-positive cells in treated tumors. Statistical analysis was carried out by Student's t-test. ✻; < 0.05, ✻✻; < 0.01

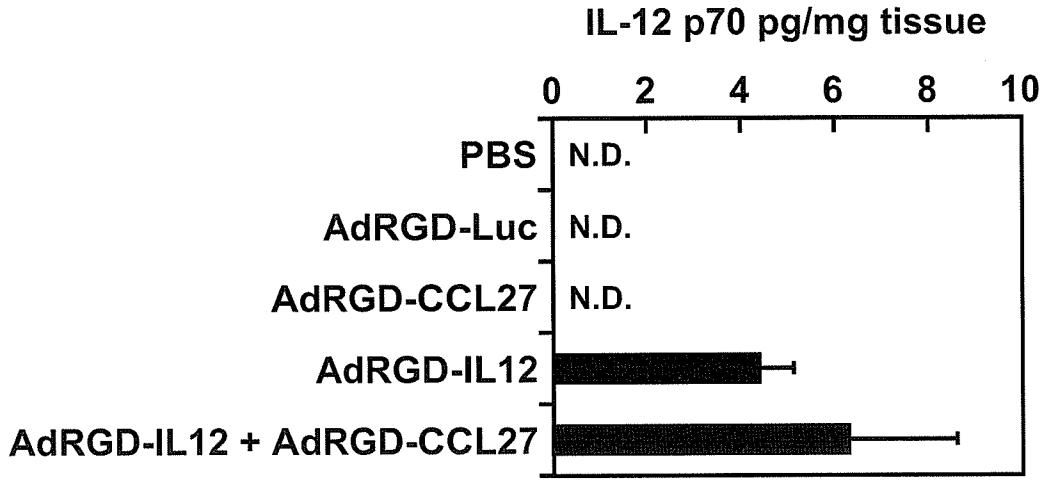

Fig. 15. IL-12 production levels in Meth-A tumors injected with AdRGD-IL12 alone or combined with AdRGD-CCL27. BALB/c mice were intradermally inoculated with 2×10^6 Meth-A cells into the flank. The tumors (9-10 mm in diameter) were injected with AdRGD-Luc alone, AdRGD-CCL27 alone, AdRGD-IL12 alone, or AdRGD-IL12 plus AdRGD-CCL27 in a ratio of 9:1 at the same dose totaling 2×10^7 PFU. PBS was injected into the tumors as a control. Two days later, the tumors were harvested, and then IL-12p70 levels in their homogenates were measured by ELISA. The data represent the mean ± SD of results from three tumors. N.D.: not detectable.

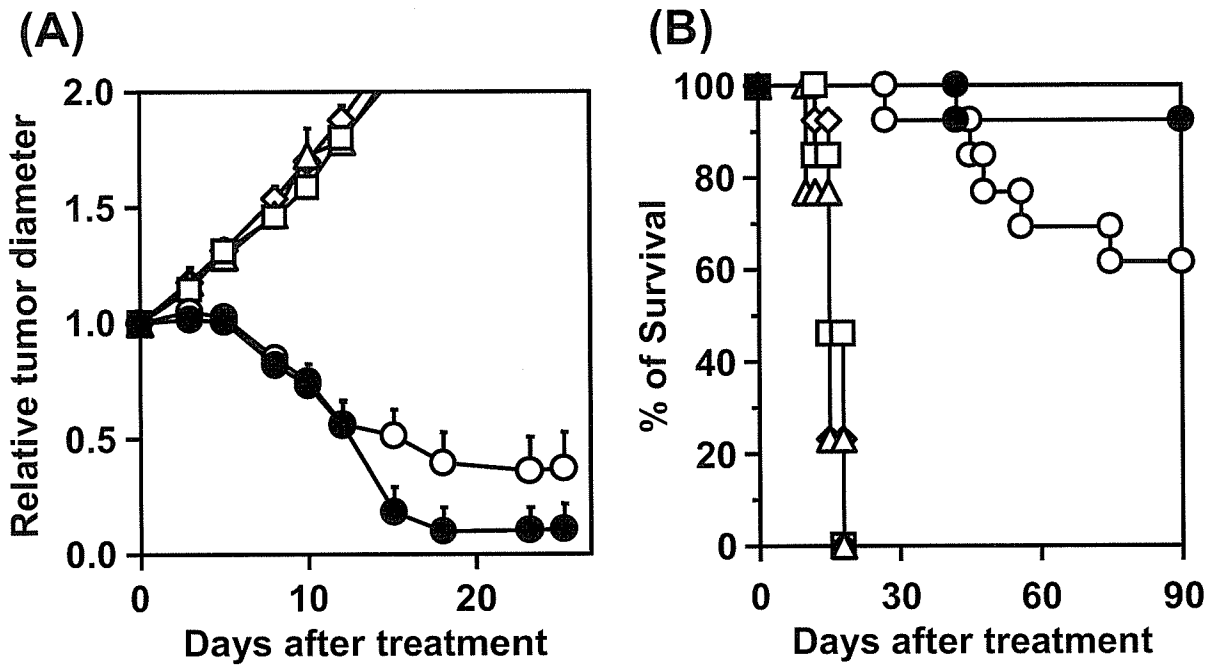

Fig. 16. Antitumor efficacy of intratumorally injected AdRGD-IL-12 plus AdRGD-CCL27 in Meth-A tumor model. BALB/c mice were intradermally inoculated with 2×10^6 Meth-A cells into the flank. The tumors (7-9 mm in diameter) were injected with either AdRGD-Luc alone (△), AdRGD-IL-12 alone (○), AdRGD-CCL27 alone (□), or the combination of AdRGD-IL-12 and AdRGD-CCL27 in a ratio of 9:1 (●) at the same dose totaling 2×10^7 PFU. PBS (◇) was injected into the tumors as a control. (A): The sizes of growing tumors were measured twice a week using microcalipers. Data are expressed as the ratio to the initial tumor diameter. Each point represents the mean ± SE of results from 7 or 8 mice. (B): Data represent the number of mice for which tumors were smaller than 20 mm, expressed as a percentage of the total mice tested in each group.

Table 3. Induction of long-term specific immunity in mice which could achieve complete regression of the primary Meth-A tumor by intratumoral injection with either AdRGD-IL12 alone or the combination of AdRGD-IL12 and AdRGD-CCL27.

Groups	Rechallenging cells[a)]	Tumor-rejected mice/ tested mice
Intact mice	Meth-A	0/10
	CT26	0/5
Meth-A-regressed mice by the injection with AdRGD-IL12	Meth-A	9/9
	CT26	0/6
Meth-A-regressed mice by the injection with AdRGD-IL12 + AdRGD-CCL27	Meth-A	12/12
	CT26	0/5

[a)] Meth-A or CT26 cells were inoculated at 10^6 or 10^5 cells/mouse, respectively.

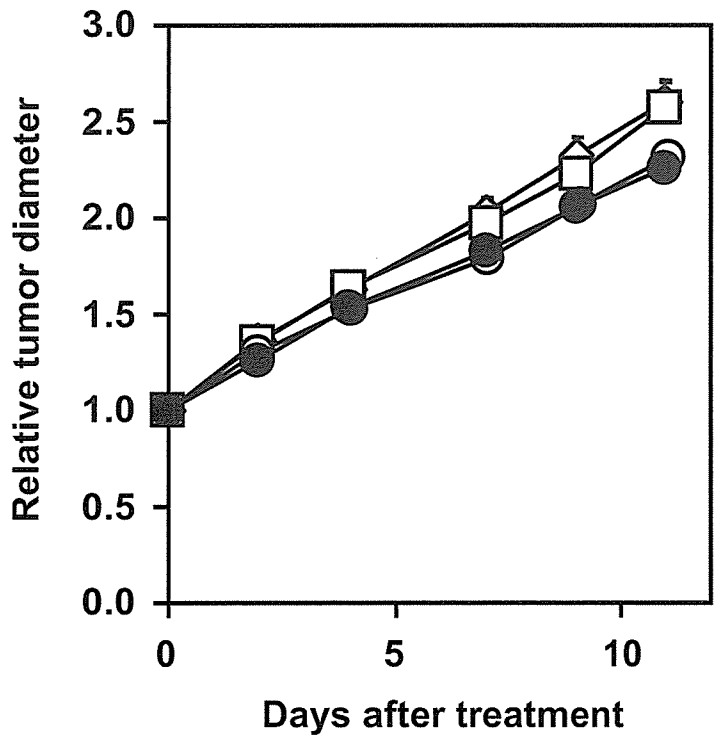

Fig. 17. Growth of Meth-A tumors injected with the AdRGD-IL-12 and AdRGD-CCL27 combination in athymic BALB/c nude mice. BALB/c nude mice were intradermally inoculated with 2×10^6 Meth-A cells into the flanks. The tumors (7-9 mm in diameter) were injected with AdRGD-Luc alone (□), AdRGD-IL12 alone (○), or AdRGD-IL12 plus AdRGD-CCL27 in a ratio of 9:1 (●) at the same dose totaling 2×10^7 PFU. PBS (△) was injected into the tumors as a control. The sizes of growing tumors were measured using microcalipers. Data are expressed as the ratio to the initial tumor diameter. Each point represents the mean ± SE of results from at least six mice.

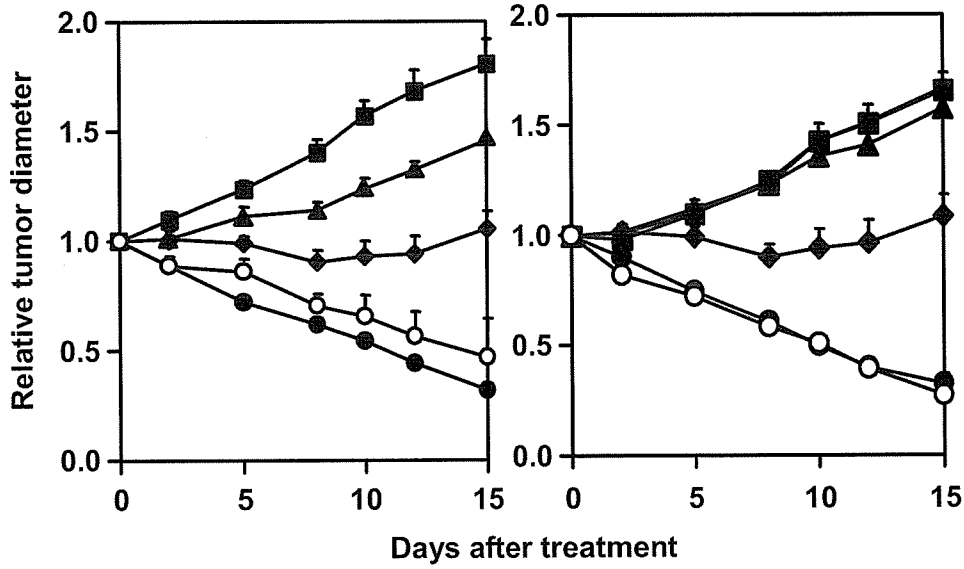

Fig. 18. Determination of immune subsets responsible for the antitumor efficacy induced by the IL-12/CCL27 combination. On day -7, BALB/c mice were intradermally inoculated with 2×10^6 Meth-A cells into the flanks. For depletion of $CD4^+$ T cells (●), $CD8^+$ T cells (▲), or NK cells (◆) in the mice, GK1.5 ascites (anti-CD4), 53-6.72 ascites (anti-CD8), or anti-asialoGM1 antisera were intraperitoneally injected on days -3, -2, -1, 0, 5, 10, and 15. Likewise, for depletion of both $CD4^+$ and $CD8^+$ T cells (■), mice were injected with GK1.5 ascites and 53-6.72 ascites. Normal rat serum (○) was injected into the mice as a control. On day 0, Meth-A tumors received the AdRGD-IL12/AdRGD-CCL27 combination intratumoral injection in a ratio of 9:1 totaling 2×10^7 PFU. Tumor growth was monitored twice a week. Data are expressed as the ratio to the initial tumor diameter. Each point represents the mean ± SE of results from 5-7 mice.

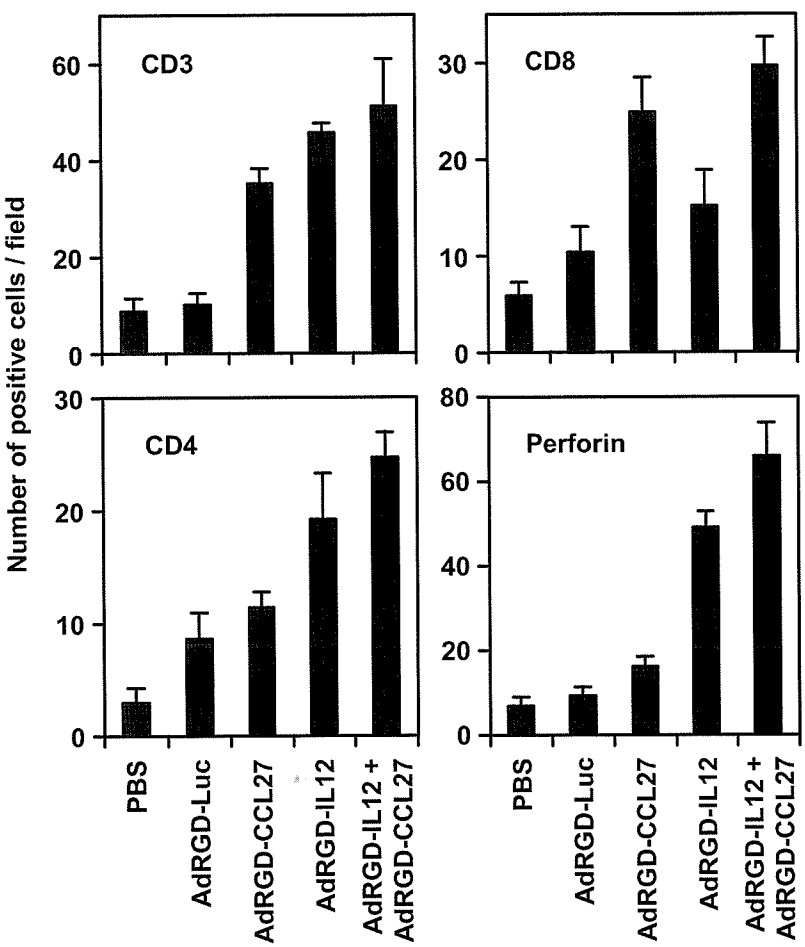

Fig. 19. Quantification of tumor-infiltrating T cell subsets and perforin-positive cells in Meth-A tumors injected with the IL-12/CCL27 combination. Meth-A cells were intradermally inoculated into the flanks of BALB/c mice at 2×10^6 cells/mouse. The tumors (7-9 mm in diameter) were injected with AdRGD-Luc alone, AdRGD-CCL27 alone, AdRGD-IL12 alone, or the AdRGD-IL12 and AdRGD-CCL27 combination in a ratio of 9:1 at the same dose totaling 2×10^7 PFU. PBS was injected into the tumors as a control. On day 6 after the intratumoral injections, immunohistochemical staining against CD3, CD4, and CD8 was performed using frozen tumor sections. These immunohistochemical sections were used to assess the numbers of $CD3^+$, $CD4^+$, $CD8^+$, and $perforin^+$ cells infiltrating into tumor parenchyma by counting six fields per specimen under ×400-magnification. The data represent the mean ± SD of results from three tumors.

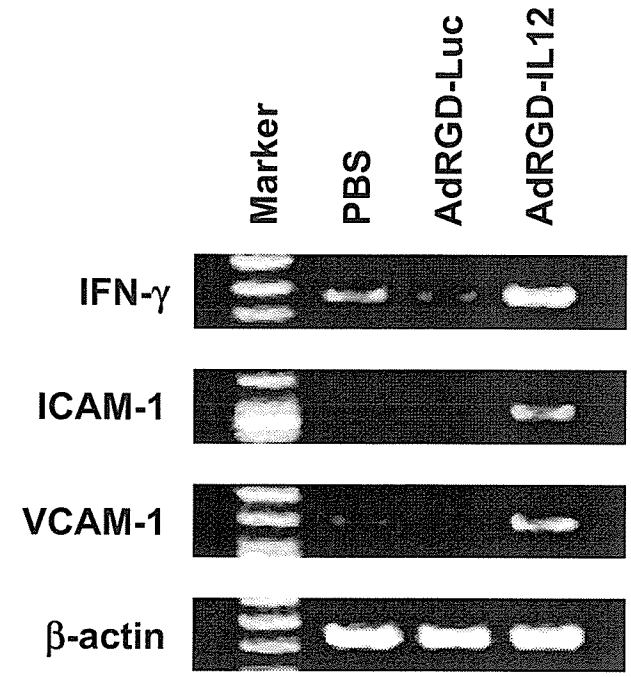

Fig. 20. Increases in expression levels of IFN-γ, ICAM-1, and VCAM-1 in Meth-A tumors injected with AdRGD-IL12. Meth-A cells were intradermally inoculated into the flanks of BALB/c mice at 2×10^6 cells/mouse. The tumors (7-9 mm in diameter) were injected with AdRGD-Luc or AdRGD-IL12 at 2×10^7 PFU. PBS was injected into the tumors as a control. On day 6 after the intratumoral injections, total RNA was isolated from the Meth-A tumors collected from treated mice, and then RT-PCR, specific for IFN-γ, ICAM-1, VCAM-1, and β-actin transcripts, was performed using each primer set descrived in Table 1. The PCR products were electrophoresed through a 2% agarose gel, stained with ethidium bromide, and visualized under ultraviolet light.

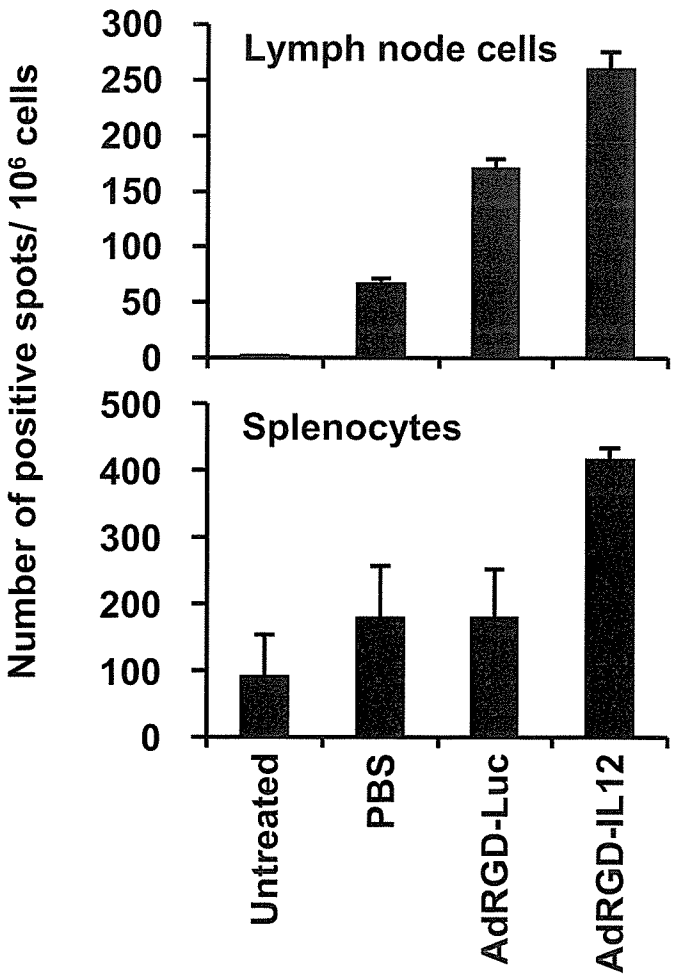

Fig. 21. The frequency of IFN-γ producing cells in draining lymph node cells and splenocytes from Meth-A-bearing mice injected with AdRGD-IL12. BALB/c mice were intradermally inoculated with 2×10^6 Meth-A cells into the flanks. The tumors (7-9 mm in diameter) were injected with AdRGD-Luc or AdRGD-IL12 at 2×10^7 PFU. PBS was injected into the tumors as a control. On day 6 after the intratumoral injections, the draining lymph node cells and splenocytes were prepared from these mice, and then were restimulated *in vitro* with mitomycine C-inactivated Meth-A cells for 24 h. IFN-γ producing cells were evaluated using mouse IFN-γ ELISPOT assay. The data represent the mean ± SE of the results from three mice.

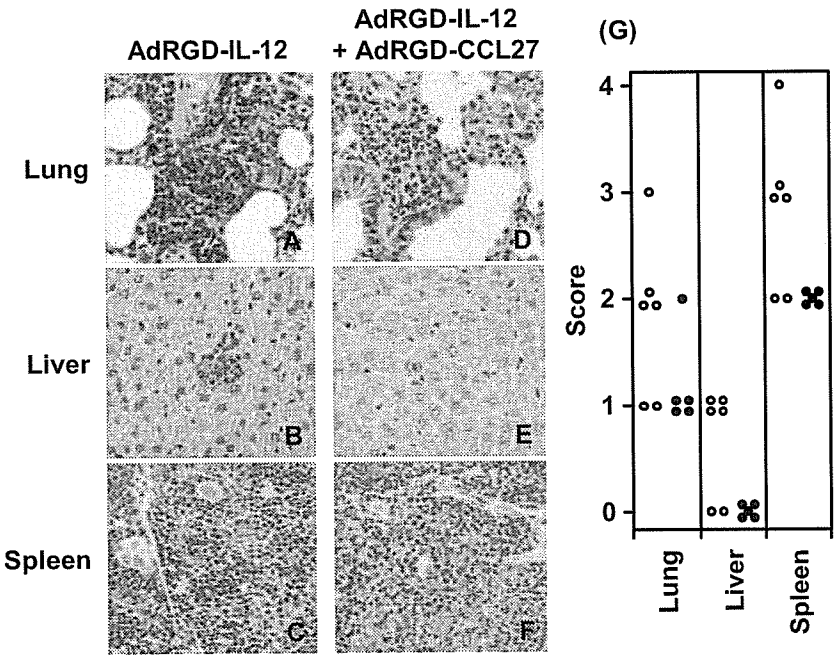

Fig. 22. Histopathological examination of lung, liver, and spleen in Meth-A tumor-bearing mice treated with the AdRGD-IL12/AdRGD-CCL27 combination intratumoral injection. BALB/c mice were intradermally inoculated with 2×10^6 Meth-A cells into the flanks. The tumors (7-9 mm in diameter) were injected with AdRGD-IL12 alone or the AdRGD-IL12 and AdRGD-CCL27 combination in a ratio of 9:1 at the same dose totaling 2×10^7 PFU. Three months later, lung (A and D), liver (B and E), and spleen (C and F) were harvested from mice in which the primary tumors were judged to have completely regressed, and then HE staining was performed using paraffin-embedded tissue sections. Original magnifications are ×300. (G): Histopathological changes (lymphocyte infiltration in lung and extramedullary hematopoiesis in liver and spleen) were scored as: 0, no; 1, rare; 2, mild; 3, moderate; 4, severe. (○); AdRGD-IL12 alone, (●); AdRGD-IL12 plus AdRGD-CCL27.

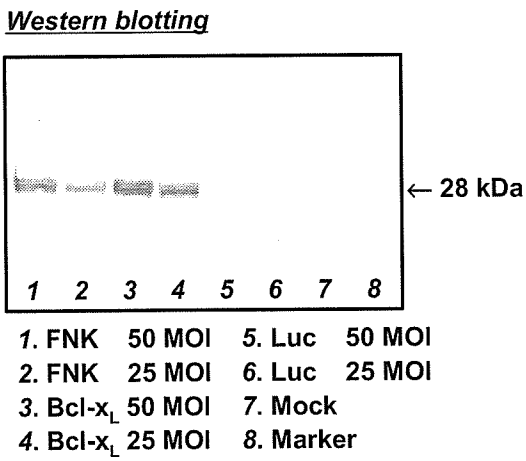

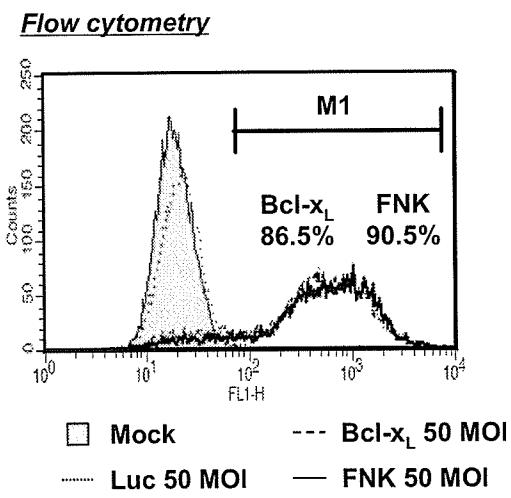

Fig. 23. Gene expression analysis in A549 cells transfected with AdRGD-Bclx$_L$ or AdRGD-FNK. Human A549 cells were transfected with AdRGD-Bclx$_L$, AdRGD-FNK, or AdRGD-Luc at 50 MOI. After 48 h-culutivation, the expression of Bcl-x$_L$ or Bcl-xFNK proteins was assessed by both western blotting and flow cytometry analysis with an intracellular staining method. The % values in the lower panel express the percentage of M1-gated cells.

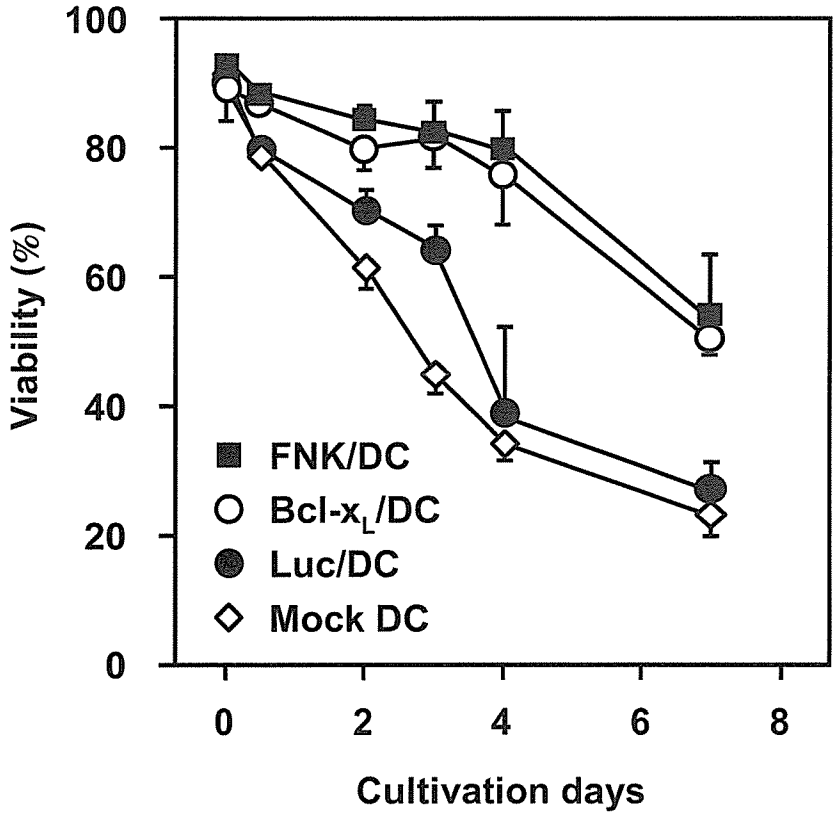

Fig. 24. *In vitro* viability of DCs transfected with AdRGD-Bclx$_L$ or AdRGD-FNK. FNK/DCs, Bcl-x$_L$/DCs, and Luc/DCs were prepared using corresponding vectors at 25 MOI, and then these transduced cells and mock DCs were cultured without cytokines and growth factors. The viability of DCs was assessed by propidium iodide staining at indicated cultivation days. Each point represents the means ± SE of triplicate cultures.

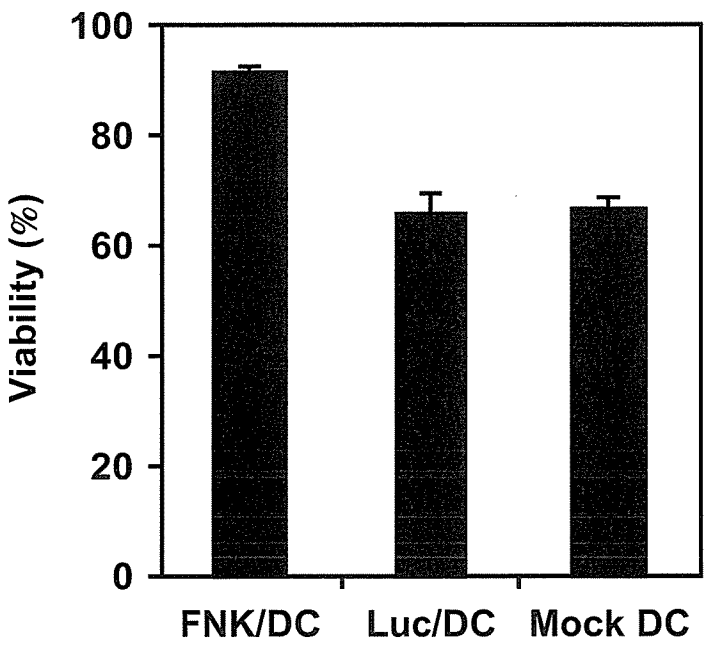

Fig. 25. The resistance of FNK/DCs to apoptosis induced by staurosporine. DCs were transfected with AdRGD-FNK or AdRGD-Luc at 50 MOI. After 48 h-cultivation, the transduced cells were cultured in the presence of 100 nM staurosporine for additional 24 h. The viability was assessed by MTT assay. Data are expressed as means ± SD of triplicate culture.

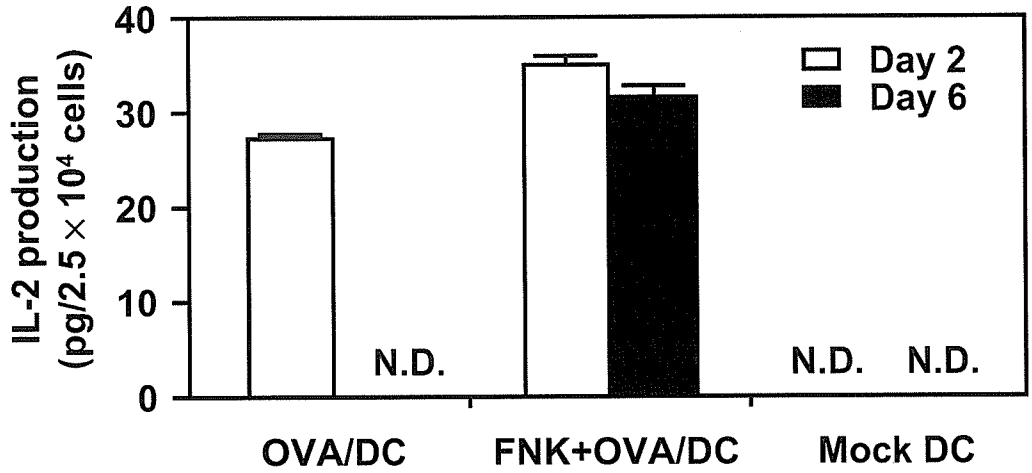

Fig. 26. Duration of antigen presentation in FNK/DCs. DCs were transfected with AdRGD-OVA alone (50 MOI) or the combination of AdRGD-OVA (50 MOI) and AdRGD-FNK (50 MOI) for 2 h. These transduced cells and mock DCs were cultured without cytokines and growth factors. On days 2 and 6, the levels of OVA-peptide presentation via MHC class I molecules on the transduced DCs were determined by bioassay using CD8-OVA1.3 cells. The data represents the means ± SD of three independent cultures. N.D.: IL-2 secreted from CD8-OVA1.3 cells was not detectable.

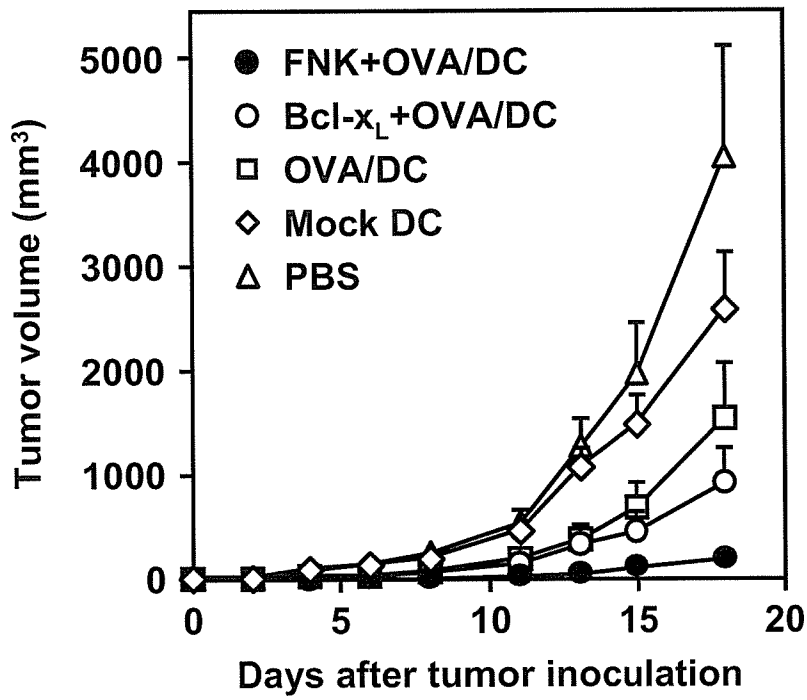

Fig. 27. Vaccine efficacy of DCs co-transduced with OVA gene and either Bcl-x_L or Bcl-xFNK gene against E.G7-OVA challenge. FNK+OVA/DCs, Bcl-x_L+OVA/DCs, and OVA/DCs were prepared using corresponding vectors at 25 MOI, and then cultures for 24 h. C57BL/6 mice were immunized by intradermal injection of transduced DCs into right flank at 5×10^4 cells. One week later, 10^6 E.G7-OVA cells were intradermaly inoculated into the left flank of these mice. The size of tumors was assessed using microcalipers three times per week. Each point represents the mean ± SE from 5-10mice.

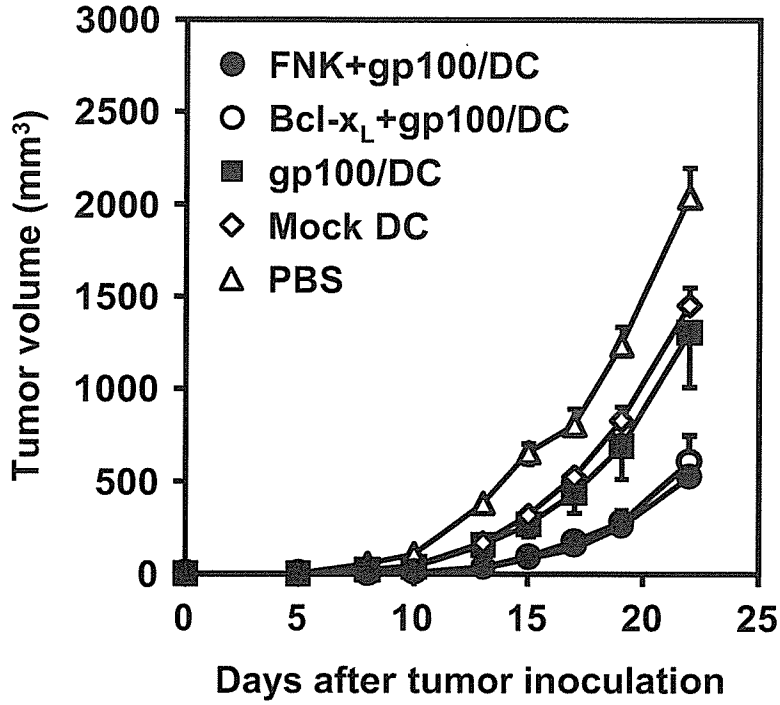

Fig. 28. Vaccine efficacy of DCs co-transduced with gp100 gene and either Bcl-x_L or Bcl-xFNK gene against B16BL6 challenge. FNK+gp100/DCs, Bcl-x_L+gp100/DCs, and gp100/DCs were prepared using corresponding vectors at 25 MOI, and then cultures for 24 h. C57BL/6 mice were immunized by intradermal injection of transduced DCs into right flank at 1.5×10^6 cells. One week later, 5×10^4 B16BL6 cells were intradermaly inoculated into the left flank of these mice. The size of tumors was assessed using microcalipers three times per week. Each point represents the mean ± SE from 5-10mice.

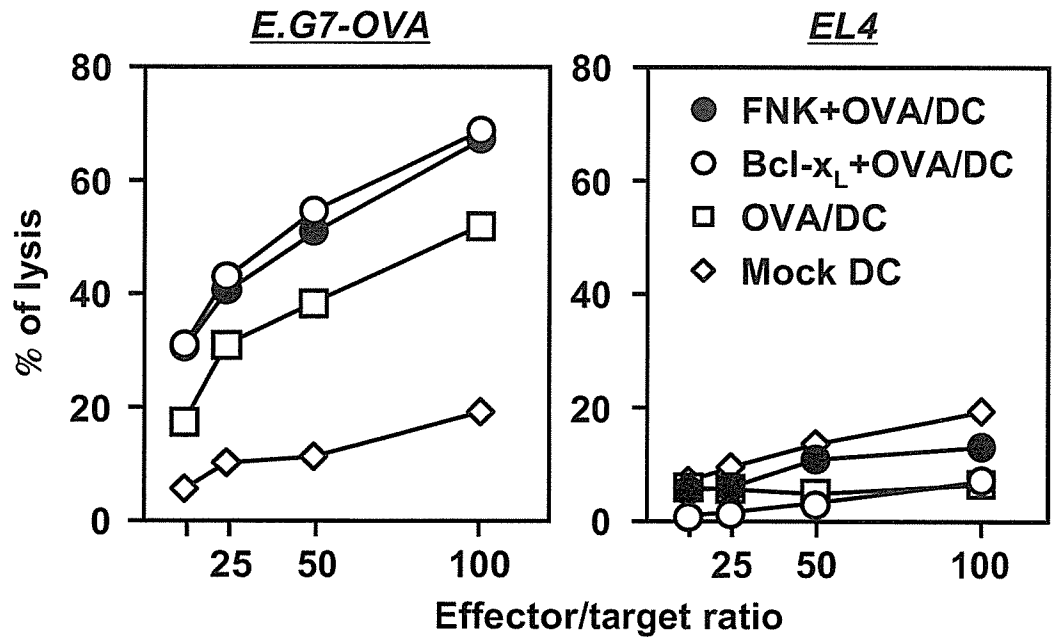

Fig. 29. OVA-specific CTL response in mice immunized with DCs cotransduced with OVA gene and either Bcl-x_L or Bcl-xFNK gene. FNK+OVA/DCs, Bcl-x_L+OVA/DCs, and OVA/DCs were prepared using corresponding vectors at 25 MOI, and then culture for 24 h. These transduced cells and mock DCs were vaccinated once intradermally into C57BL/6 mice at 2.5×10^4 cells. At 1 week after immunization, splenocytes were prepared from these mice, and were re-stimulated *in vitro* for 5 days with mitomycine C- inactivated E.G7-OVA cells. Cytolytic effects of re-stimulated splenocytes (effector cells) against E.G7-OVA or EL4 cells (target cells) were evaluated by ^{51}Cr-release assay.

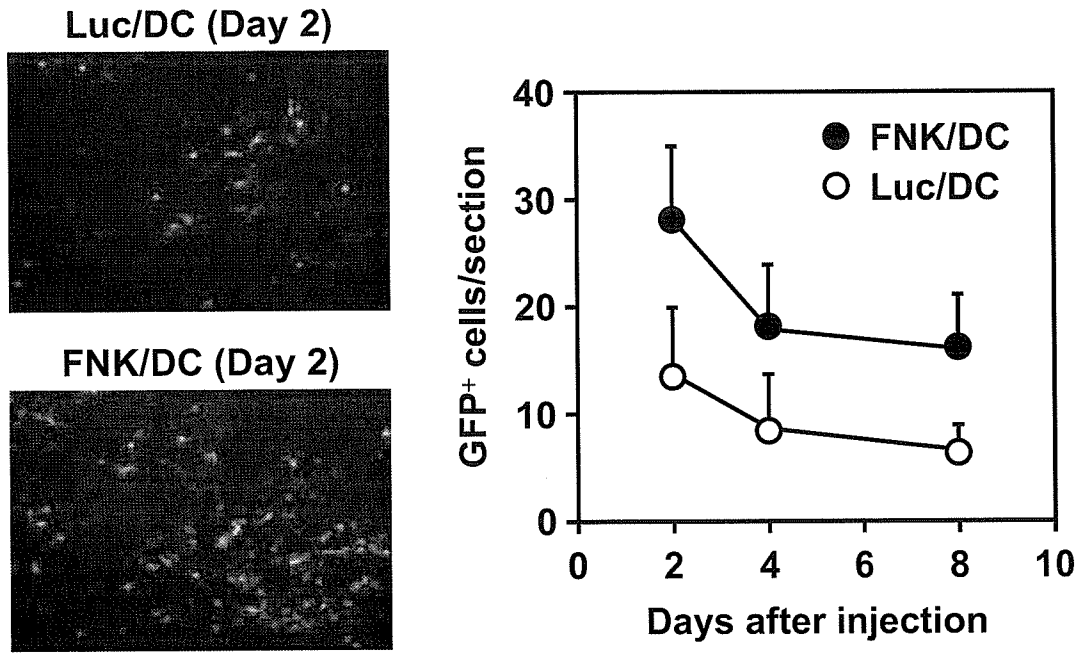

Fig. 30. Enhanced accumulation of FNK/DCs from administration site to regional lymph node. DCs derived from GFP transgenic mice were transfected with AdRGD-FNK or AdRGD-Luc at 25 MOI, and then were cultured for 24 h. These transduced GFP^+ DCs were injected intradermally into right flank of wild type C57BL/6 mice at 2×10^6 cells. The draining inguinal lymph nodes were harvested on days 2, 4, and 6 after injection. Frozen sections (6-μm thickness) of lymph node were prepared, and then the number of GFP^+ DCs was counted under fluorescence microscopy. Each point represents the mean ± SE of results from three mice.

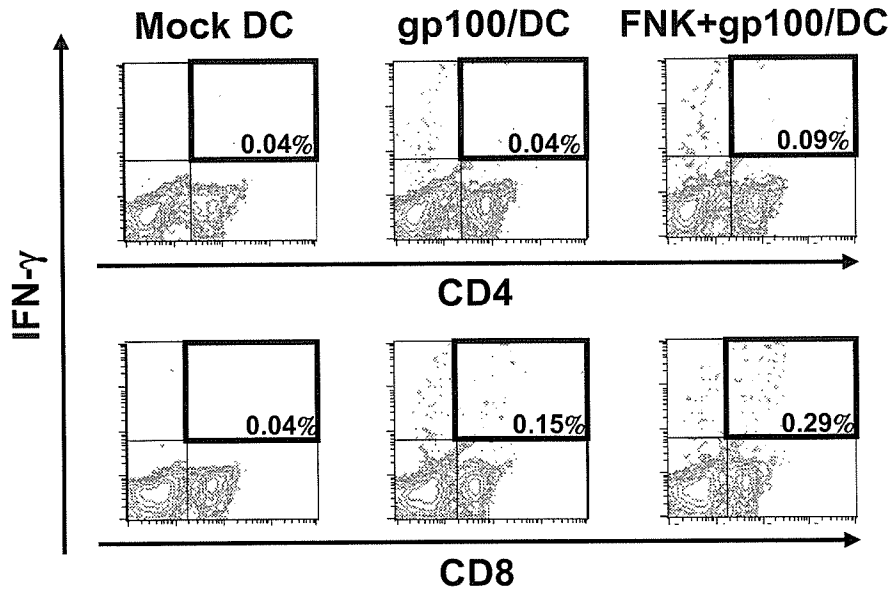

Fig. 31. gp100-specific $CD4^+$ or $CD8^+$ T cell immune response in mice immunized with DCs cotransduced with gp100 and Bcl-xFNK genes. gp100/DCs and FNK+gp100/DCs were prepared using corresponding vectors at 25 MOI, and then culture for 24 h. These transduced cells and mock DCs were vaccinated once intradermally into C57BL/6 mice at 1.5×10^6 cells. At 1 week after immunization, regional lymph node cells were prepared from these mice, and were re-stimulated *in vitro* with mitomycine C- inactivated B16BL6 cells for 24 h. The number of IFN-γ-producing $CD4^+$ or $CD8^+$ T cells was analyzed by intracellular IFN-γ staining followed by flow cytometry.

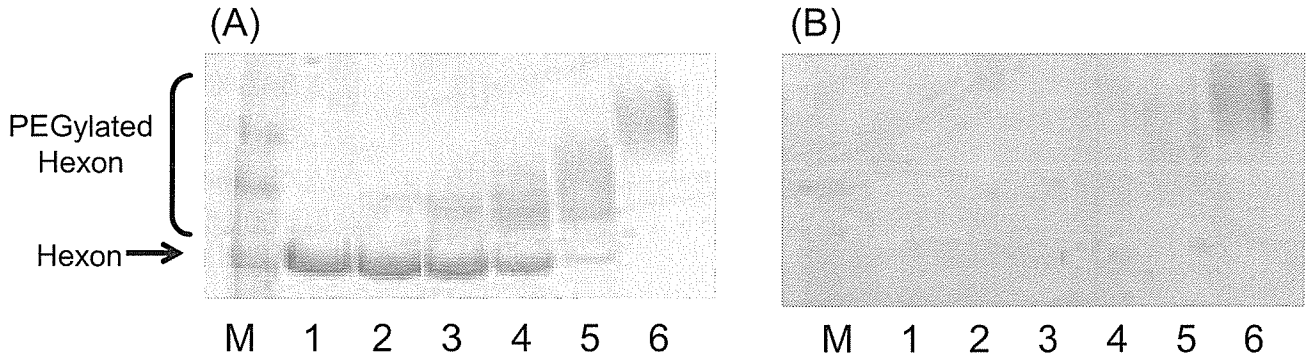

Fig. 32. SDS-PADE analysis of PEGylated adenovirus vectors. Comparison of two SDS-gels (A, B) that were run under identical conditions and loaded as follows : lane M, protein markers ; lane 1, Ad : PEG=1:0 (unmodified-Ad) ; lane 2, 1:25 ; lane 3, 1:100 ; lane 4, 1:400 ; lane 5, 1:1600 ; lane 6, 1:6400. (A) The gel was stained with Coomassie blue. (B) The gel was stained for PEG using barium iodide.

Table 4. Relationship between degree of PEGylated-Hexon and adenovirus vector size.

Ratio (Ad:PEG)*	PEG modification ratio (%)	Vector size (nm)	Serum half-life (min)
1:0	0	113.3±0.76	1.6
1:25	10	120.6±0.64	1.8
1:100	34	123.8±0.98	1.8
1:400	61	128.5±1.25	5.0
1:1600	89	137.6±0.91	12.0
1:6400	100	148.2±1.48	78.6

* ; Amount of PEG to lysine residue of adenovirus vector capsid protein (mol : mol)

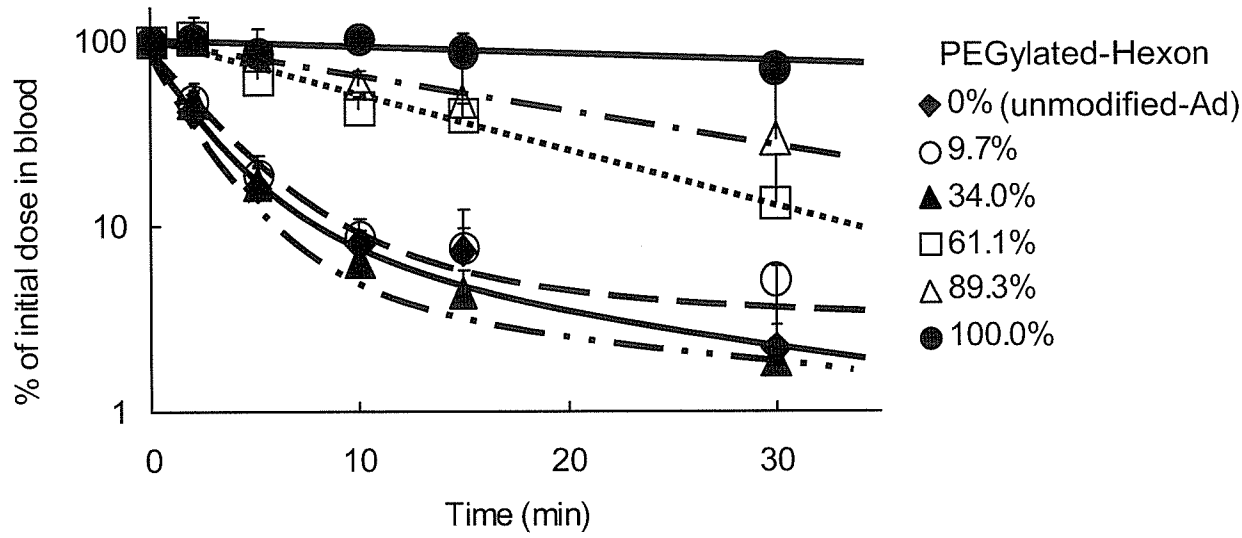

Fig. 33. Pharmacokinetics of PEGylated adenovirus vectors. Normal female BALB/c mice were administrated intravenously with $1x10^{10}$ particles of unmodified-Ad or PEG-Ads. Blood samples were drawn at different times. The concentration of adenovirus vectors in serum was quantitated with southern blot method. A standard curve was made for each PEG-Ads. Each point was represented as mean ±S.D. (n=4).

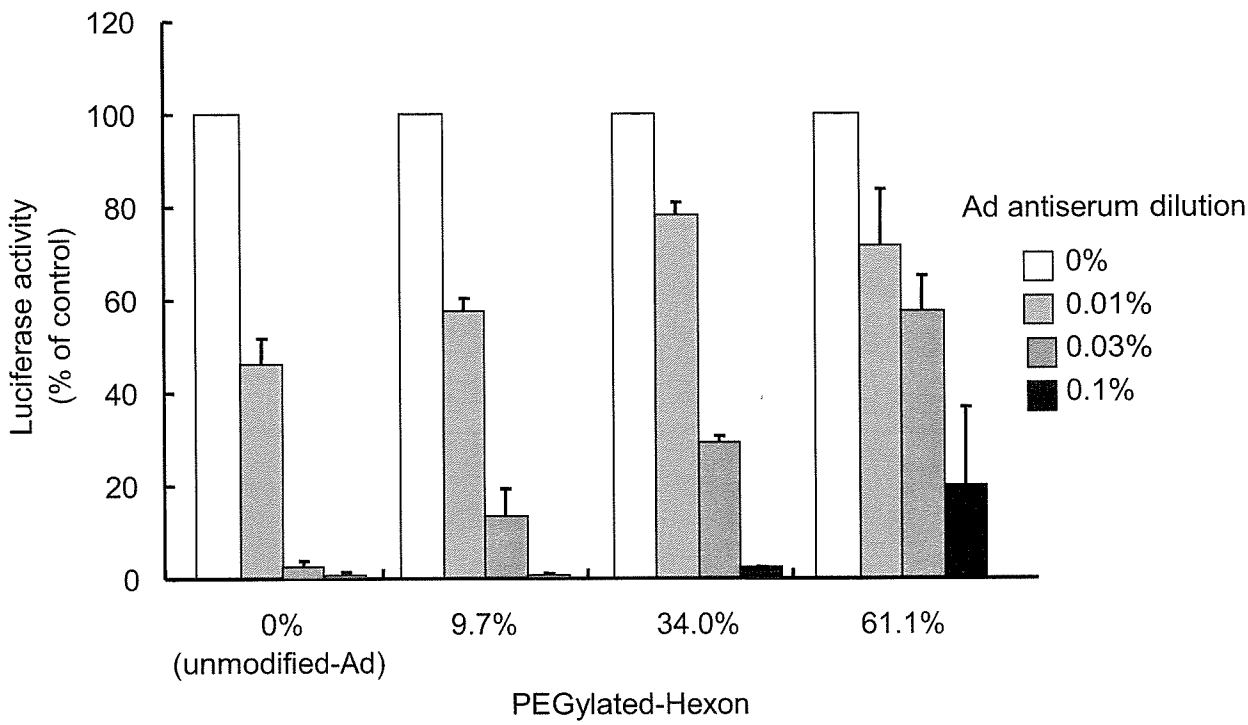

Fig. 34. Transduction of A549 cells by PEGylated adenovirus vectors in the presence or absence of adenovirus vectors antiserum. A549 cells ($1x10^4$ cells) were tranceduced with 1000 particles/cell of unmodified-Ad or PEG-Ads in the presence or absence of Ad antiserum respectively. Luciferase expression was measured after 24 hr. Each point was represented as mean ±S.D. (n=3).

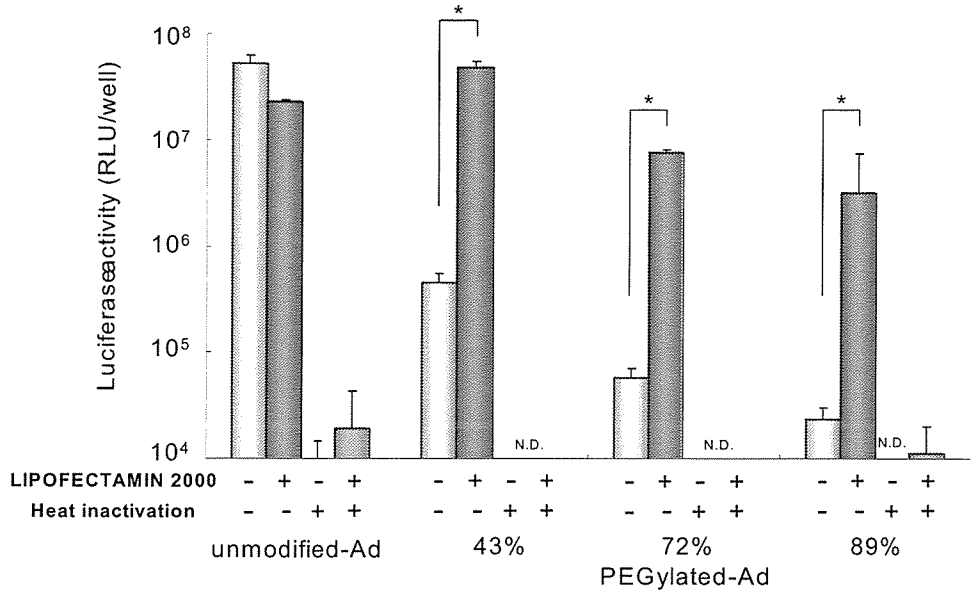

Fig. 35. Transduction efficiency of PEGylated adenovirus vectors into A549 cells in the presence or absence of LIPOFECTAMINE 2000. A549 cells ($2x10^4$ cells) were transduced with 1000 particles/cell of unmodified or PEGylated Ad-Luc in the presence or absence of 20 μ g/ml of LIPOFECTAMINE 2000. After 4 hr, the virus solution was replaced with fresh medium, and the cells were incubated for 24 hr. Luciferase expression was measured. Each point represents the mean $\pm$ S.D. (n=3). * $P<0.05$ (*t-test*).

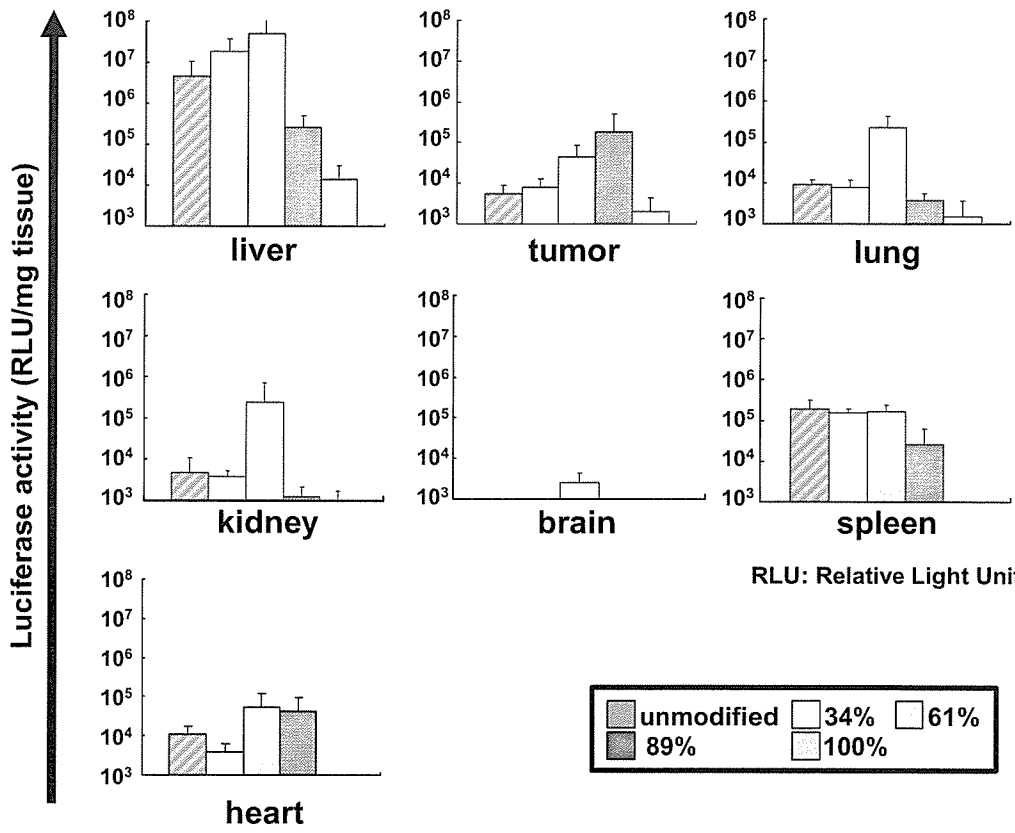

Fig. 36. *In vivo* gene expression pattern of PEG-Ad after i.v. administration into mice. 2×10^6 Meth-A fibrosarcoma tumor cells were inoculated intradermally and 10^{10} particles of unmodified or PEGylated Ad-Luc were injected intravenously after approximately one week. After 2 days, organs were harvested and homogenized with buffer. Luciferase activity was then measured using the kit according to the manufacture's instructions.(n=4).

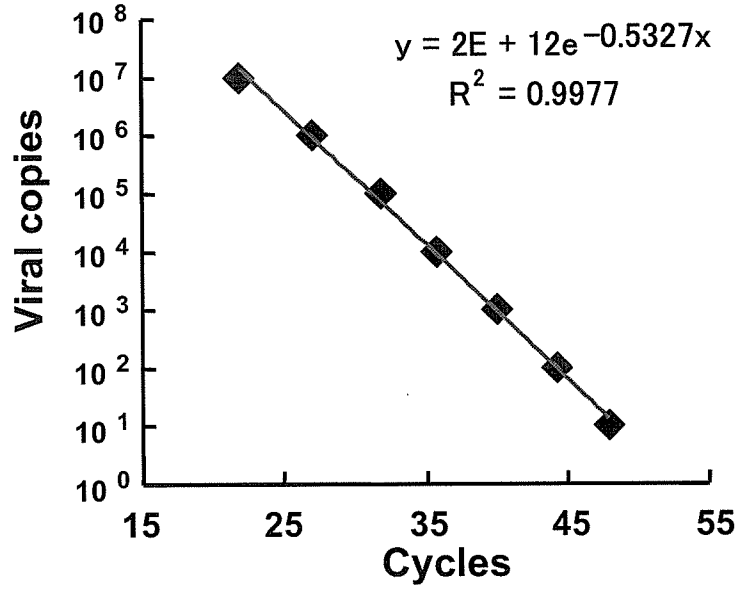

Fig. 37. Standard curve of TaqMan Real-time PCR

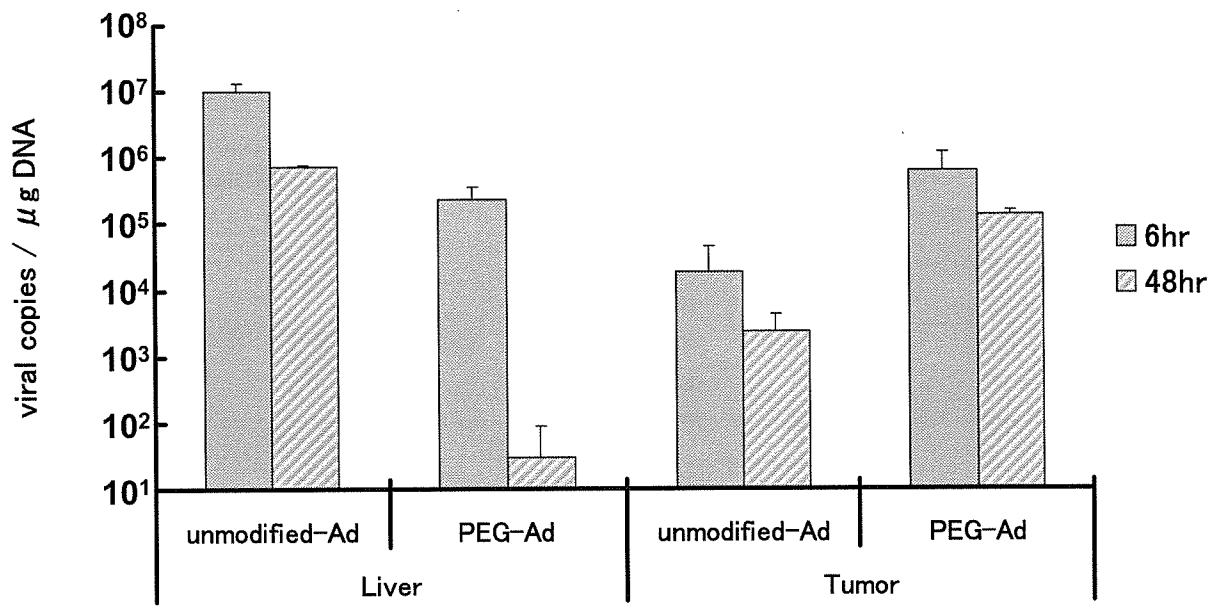

Fig. 38. Accumulation of Ad particles in tumor, and reduction in liver induced by PEGylation. Real-time PCR was carried out for detecting viral particles existence in tumor and liver 6, 48 h after systemically administration of 1 x 10^{11} VP of both unmodified-Ad and PEGylated Ad (89% of modification ratio).

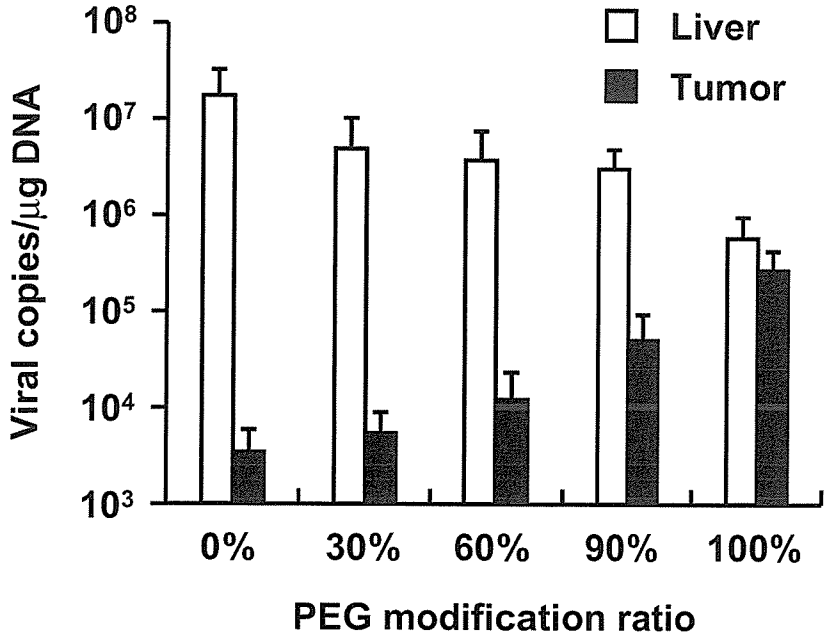

Fig. 39. Biodistribution of PEG-Ad vector in Meth-A tumor-bearing mice. BALB/c mice were intradermally inoculated with Meth-A cells into the flank at 2×10^6 cells/mouse. One week later, these mice were intravenously injected with unmodified Ad-Luc or PEG-Ad-Luc with various modification ratios at 10^{11} VP/mouse. At 6 h after vector injection, tumor and liver were harvested, and then real-time PCR was carried out for detecting viral geneme in DNA isolated from them. Data represent the mean ± SD of results from four mice.

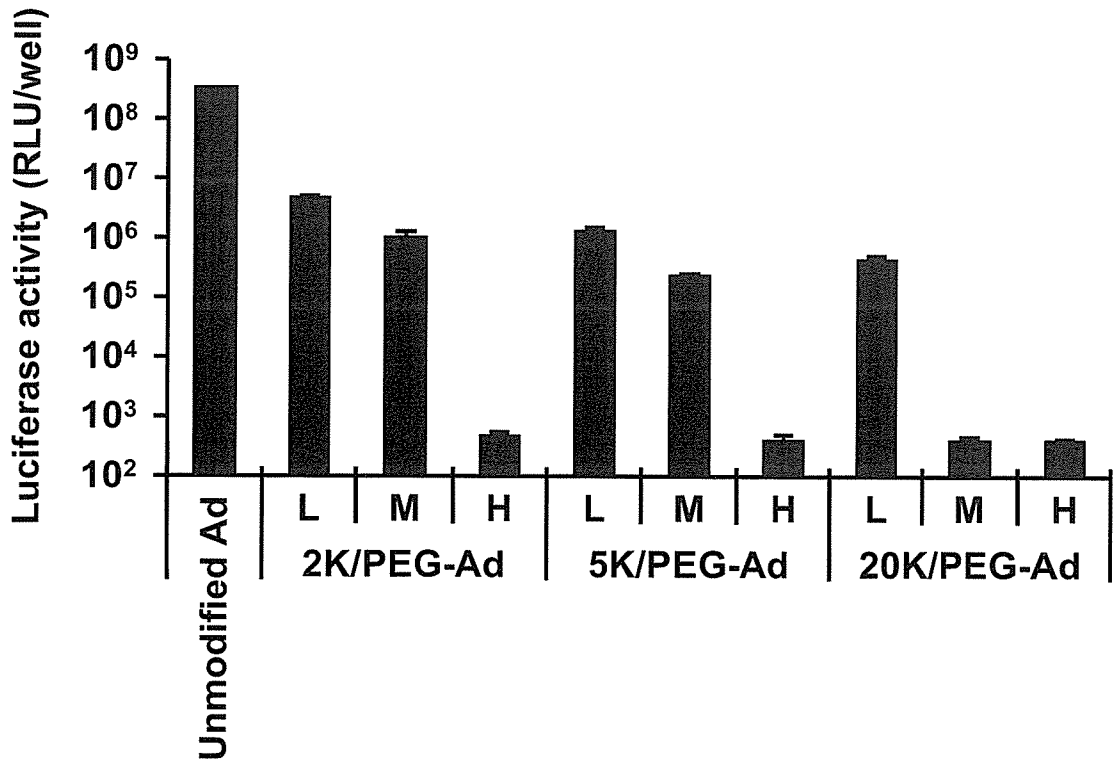

Fig. 40. Transduction efficiency of PEG-Ads modified with various PEG. A549 cells were transduced with unmodified Ad-Luc, 2K/PEG-Ad-Luc, 5K/PEG-Ad-Luc, or 20K/PEG-Ad-Luc at 10000 VP/cell. The modification ratio of PEG-Ad are indicated as follows: L, 30-40%; M, 50-60%; H, 80-90%. After 24 h-cultivation, luciferase activity was measured. Data represents the mean ± SD of results from triplicate culture.

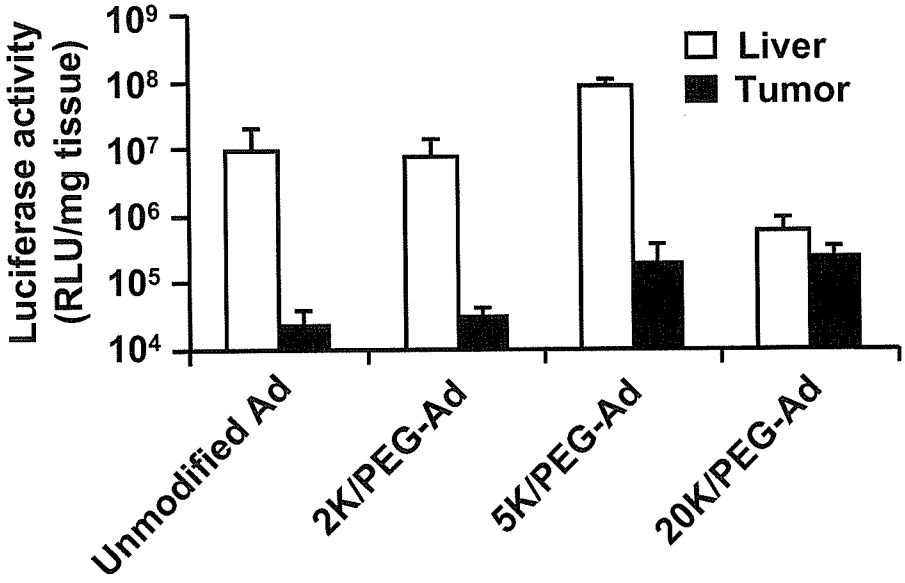

Fig. 41. *In vivo* gene expression of PEG-Ads modified with various PEG after i.v. administration into Meth-A tumor-bearing mice. Meth-A tumor-bearing BALB/c mice were intravenously injected with unmodified Ad-Luc, 2K/PEG-Ad-Luc. 5K/PEG-Ad-Luc, or 20K/PEG-Ad-Luc at 10^{10} VP/mouse. Modification ratio of each PEG-Ad was 30-40%. Two days later, liver and tumor were harvested and homogenized with buffer. Luciferase activity was measured using the kit according to the manufacture's instructions. Data represent the mean ± SD or results from five mice.

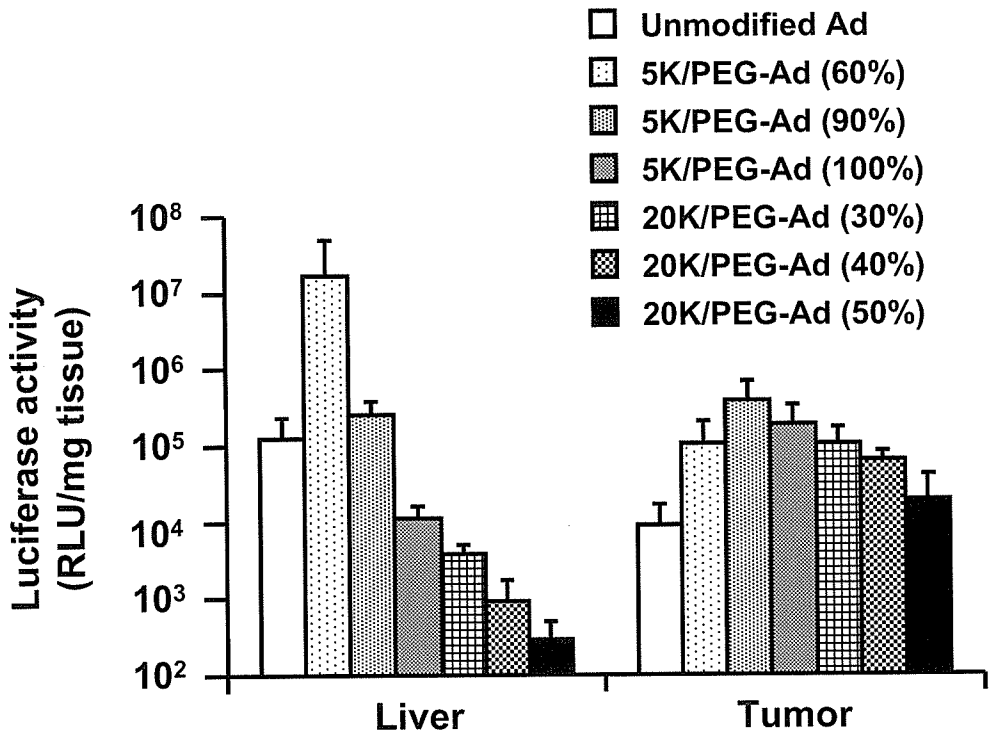

Fig. 42. Gene expression pattern in Meth-A tumor-bearing mice injected i.v. with various PEG-Ads. Meth-A tumor-bearing mice were i.v. injected with unmodified or various PEGylated Ad-Luc at 10^{10} VP. Two days later, liver and tumor were harvested and homogenized with buffer. Luciferase activity was then measured using the kit according to the manufacture's instructions. Data represent the mean ± SE of results from five mice.

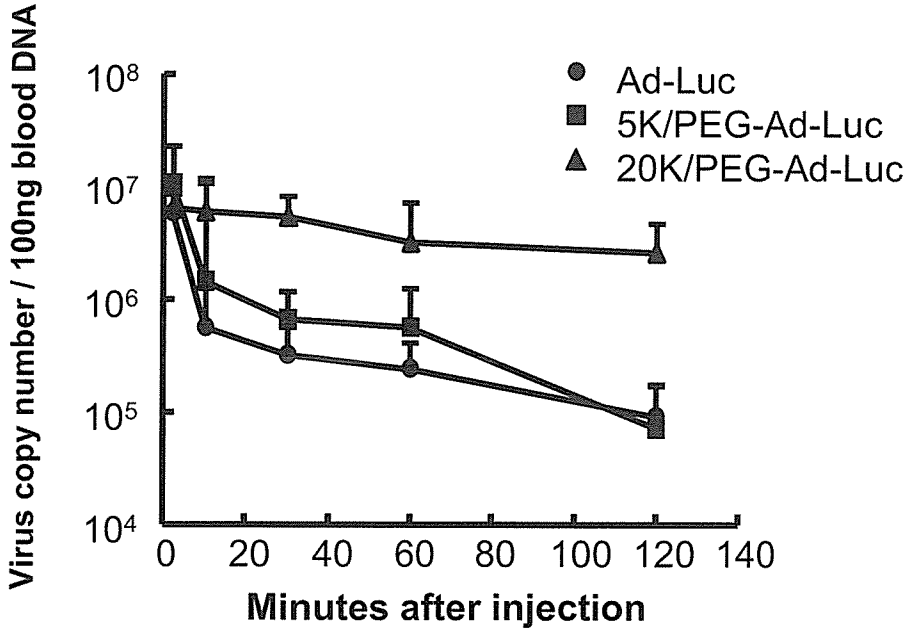

Fig. 43. Pharmacokinetics of PEG-Ads after i.v. injection. BALB/c mice were injected intravenously with unmodified Ad-Luc, 5K/PEG-Ad-Luc, or 20K/PEG-Ad-Luc at 10^{10} VP/mouse. The concentration of Ad in the blood at the indicated time points was determined by real-time quantitative PCR. Data are presented as means ± S.D. (n = 6).

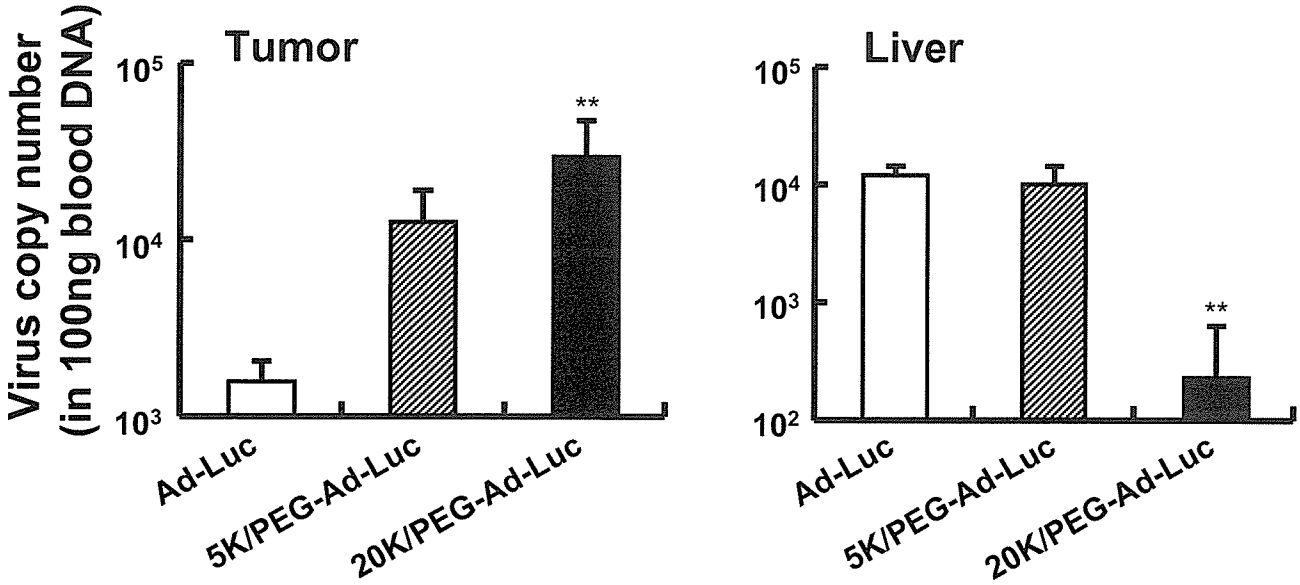

Fig. 44. Tissue distribution of PEG-Ads after i.v. injection. Once the tumor diameter was approximately 8 mm, Meth-A tumor-bearing mice were injected intravenously with 10^{10} particles of unmodified Ad-Luc or PEG-Ad-Luc. Six hours after the injection, the tumor and liver tissues were harvested and DNA extracted. The number of viral genomes in each sample was measured by real-time quantitative PCR. Data are presented as means ± S.D. (n = 4-6; **,$P < 0.01$ compared with value for unmodified Ad).

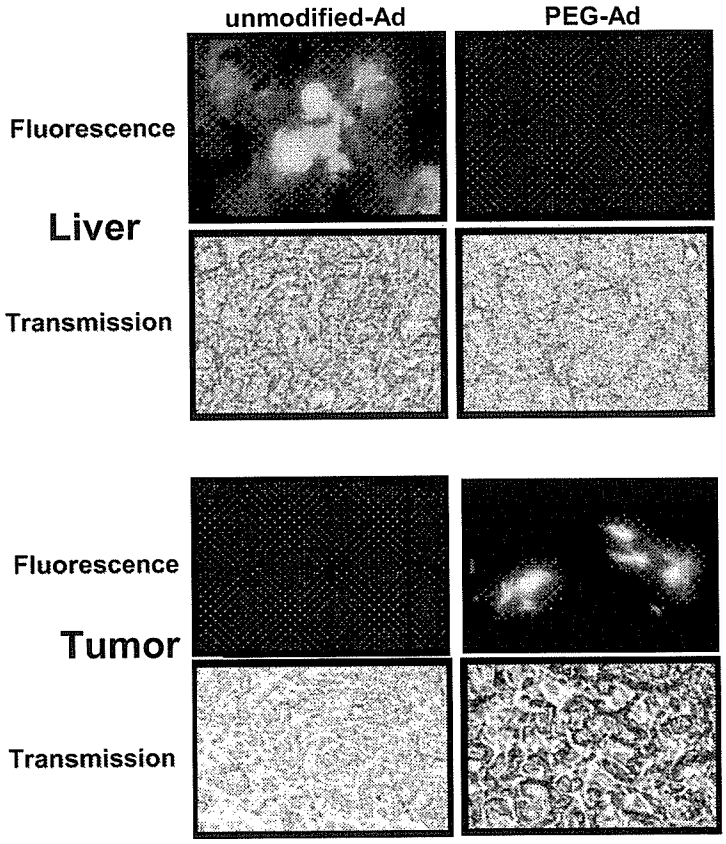

Fig. 45. EGFP gene expression of unmodified-Ad and PEG-Ad. Tumor-bearing mice were administrated intravenously with 1.5×10^{11} particles of unmodified-Ad or PEG-Ad expressing EGFP. After 48 hr, livers and tumors were removed, processed for frozen sectioning. EGFP was observed under a fluorescence microscopy at x 400 magnification.

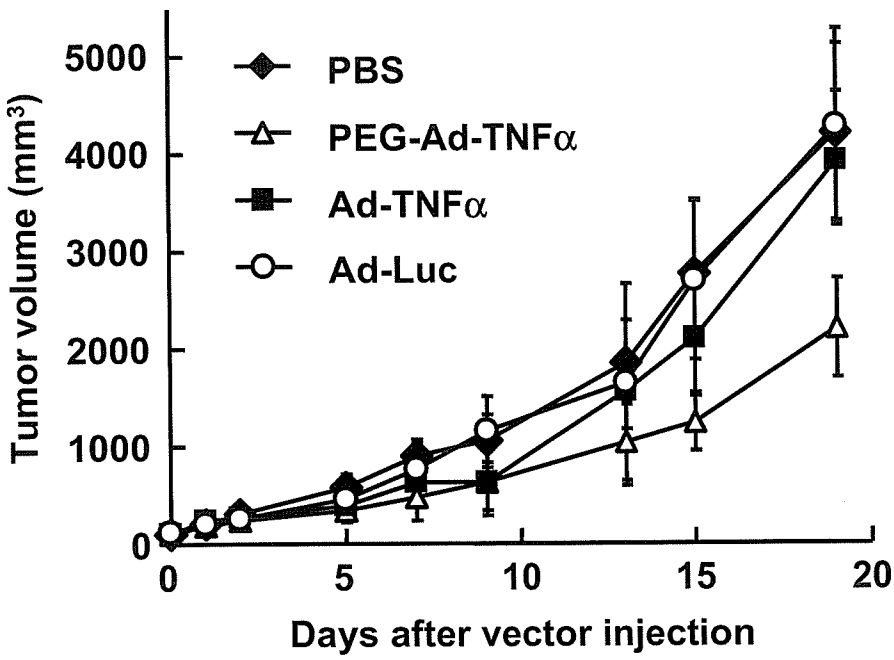

Fig. 46. Anti-tumor efficacy of systemic injection of PEG-Ad-TNFα. Meth-A tumor-bearing BALB/c mice were intravenously injected with Ad-Luc, Ad-TNFα, or PEG-Ad-TNFα (89% modification ratio) at 10^{10} VP/mouse. Tumor volume was measured two or three times per week. Each point represents the mean ± SE from 6-8 mice.

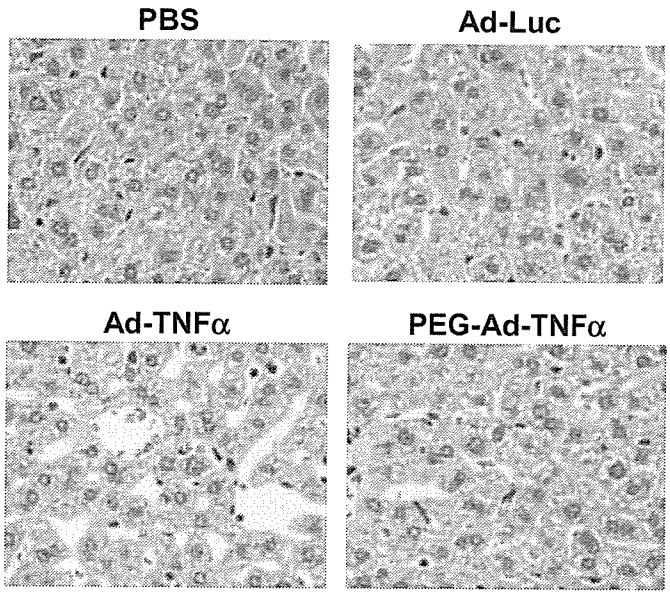

Fig. 47. Histopathological examination of liver after i.v. injection of PEG-Ad-TNFα. Meth-A tumor-bearing BALB/c mice were intravenously injected with Ad-Luc, Ad-TNFα, or PEG-Ad-TNFα (89% modification ratio) at 10^{10} VP/mouse. After 48 h, livers were harvested, placed in neutral 10% formalin, and embedded in paraffin. Sections (5-μm) were prepared for hematoxylin and eosin staining and histopathological examination. Original magnification is ×300.

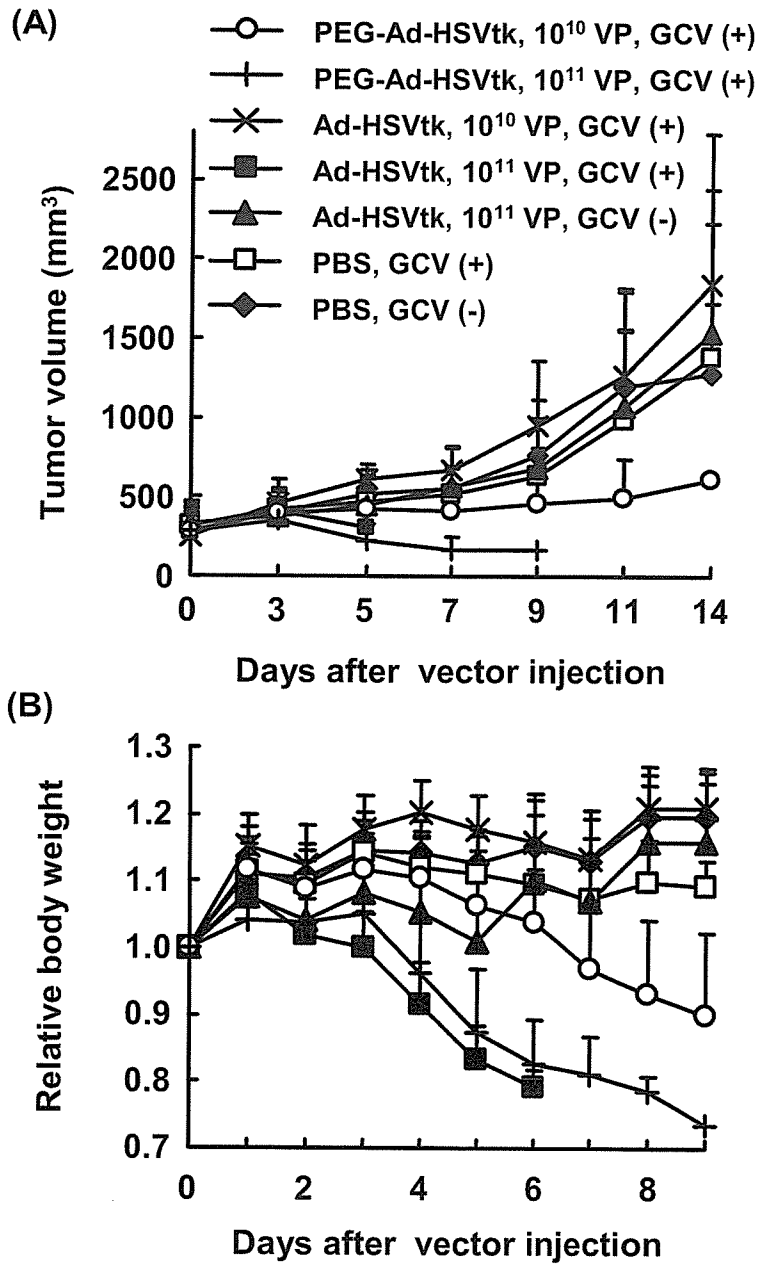

Fig. 48. Tumor growth (A) and body weight change (B) in Meth-A tumor-bearing mice treated with HSVtk/GCV system. Meth-A tumor-bearing BALB/c mice were intravenously injected with Ad-Luc, Ad-HSVtk, or PEG-Ad-HSVtk (90% modification ratio) at 10^{10} or 10^{11} VP/mouse. These mice were treated once daily with intraperitroneal injection of GCV (50 mg/kg/day) for 10 days. The tumor volume (A) and body weight (B) were monitored. Each point represents the mean ± SD of results from six mice.

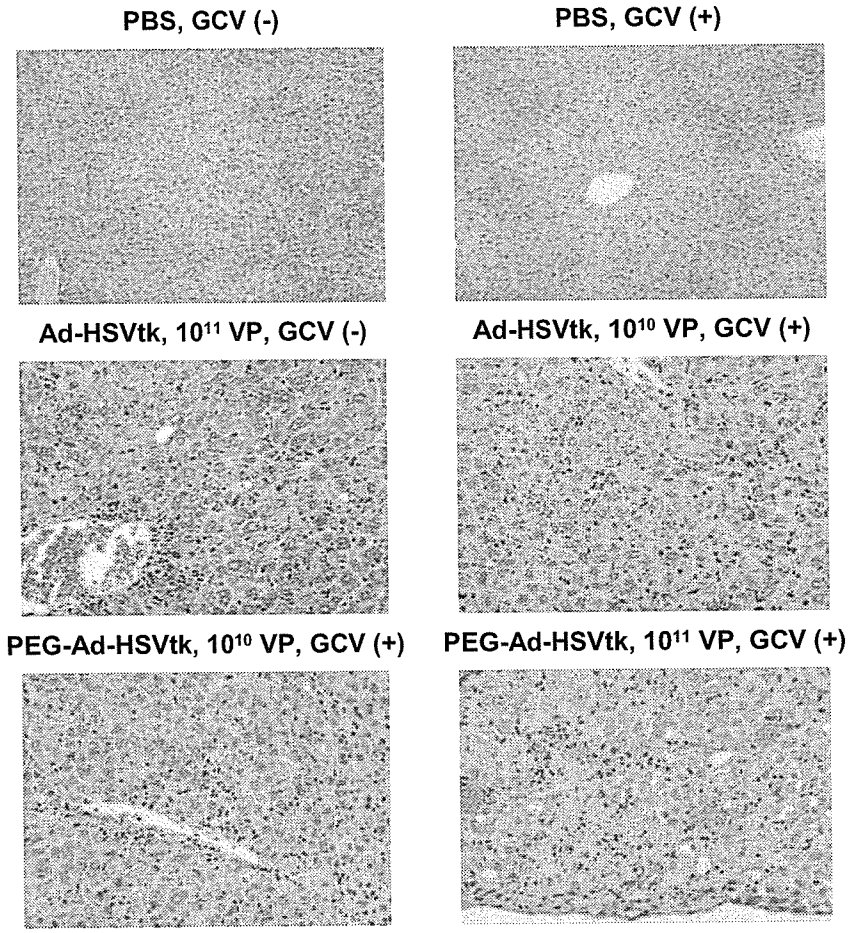

Fig. 49. Histopathological examination of liver after HSVtk/GCV treatment. Meth-A tumor-bearing BALB/c mice were intravenously injected with Ad-HSVtk or PEG-Ad-HSVtk (90% modification ratio) at 10^{10} or 10^{11} VP/mouse. These mice were treated once daily with intraperitroneal injection of GCV (50 mg/kg/day). On day 7 after vector injection, livers were harvested, placed in neutral 10% formalin, and embedded in paraffin. Sections (5-μm) were prepared for hematoxylin and eosin staining and histopathological examination. Original magnification is ×300.

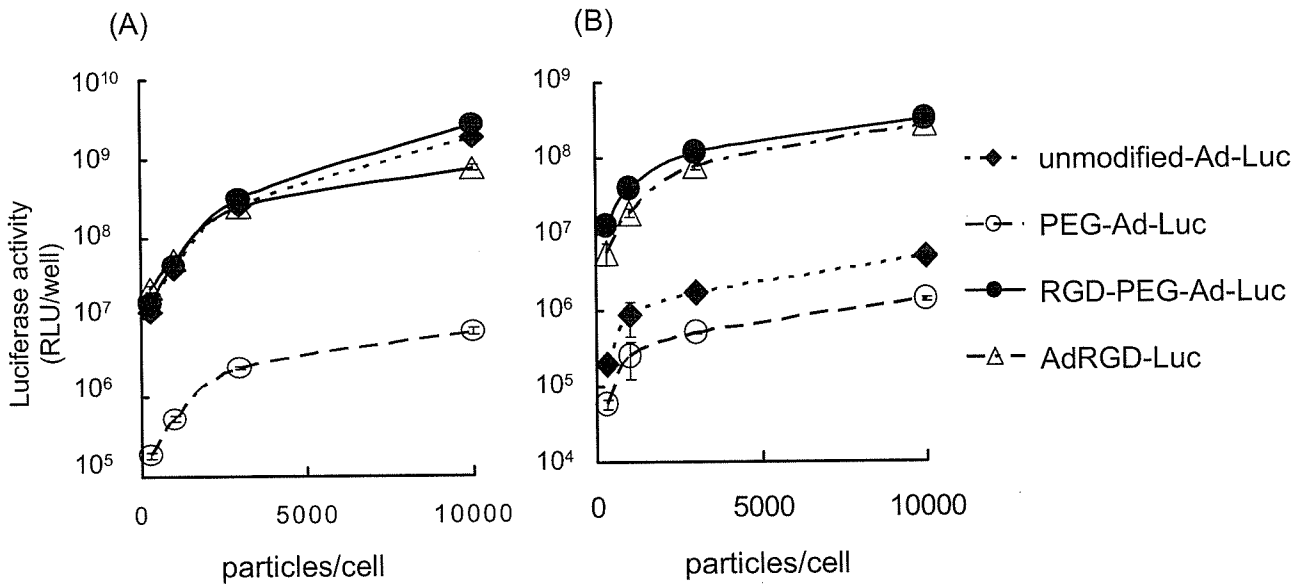

Fig. 50. Transduction of A549 cells and B16BL6 cells by RGD-PEGylated adenovirus vectors. (A) A549 cells and (B) B16BL6 cells ($2x10^4$ cells) were transfected with 300, 1000, 3000 or 10000 particles/cell of Ad, PEG-Ad-Luc, RGD-PEG-Ad-Luc or AdRGD-Luc respectively. Luciferase expression was measured after 24 hr. Each point was represented as mean ±S.D.